Algorithm to Retrieve Aerosol Optical Properties From High-Spectral-Resolution Lidar and Polarization Mie-Scattering Lidar Measurements

Tomoaki Nishizawa, Nobuo Sugimoto, Ichiro Matsui, Atsushi Shimizu, Boyan Tatarov, and Hajime Okamoto

***Abstract*—We developed an algorithm to estimate the vertical profiles of extinction coefficients at 532 nm for three aerosol types that are water-soluble, soot, and dust particles, using the extinction and backscattering coefficients at 532 nm for total aerosols derived from high-spectral-resolution lidar (HSRL) measurements and the receiving signal at 1064 nm and total depolarization ratio at 532 nm measured with Mie scattering lidar (MSL). The mode radii, standard deviations, and refractive indexes for each aerosol component are prescribed by the optical properties of aerosols and clouds database; the optical properties for each aerosol component are computed from Mie theory on the assumption that their particles are spherical and homogeneous, except for dust. To consider the effect of nonsphericity, the dust lidar ratio at 532 nm is assumed to be 50 sr, the value that is reported for Asian dust from the other observational studies. We performed sensitivity study on retrieval errors. The errors in extinction coefficient for each aerosol component were smaller than 30% and 60% when the measurement errors were ±5% and ±10%. We demonstrated the ability of the algorithm by applying to the HSRL + MSL data measured at Tsukuba, Japan. Plumes consisting of water-soluble aerosols, soot, dust, or their mixture were retrieved; these results were consistent with simulation with a global aerosol transport model. Introducing the dust lidar ratio significantly improved a correlation between the retrieved dust concentration and the aerosol depolarization ratio at 532 nm derived from HSRL + MSL than the use of spherical dust optical model in the retrieval.**

***Index Terms*—Aerosols, algorithms, geophysics, laser radar.**

I. Introduction

ACTIVE instruments such as lidar and radar are powerful tools for studying temporal and spatial variations in aerosols and clouds. Mie scattering lidar (MSL) is the most frequently used active instrument for studying aerosol optical properties. Extinction and backscattering coefficients for aerosols are derived from MSL data by assuming an extinction-to-backscattering ratio (lidar ratio). Improved aerosol observation has recently been conducted by using the lidar technology with high-spectral-resolution lidar (HSRL) (e.g., see [1]) and Raman lidar (e.g., see [2]). HSRL and Raman lidar are more useful than MSL because they can provide extinction and backscattering coefficients for total aerosols without assuming a lidar ratio. Combined use of these lidars will provide more information about aerosol properties because various kinds of data, such as extinction and backscattering coefficients and depolarization ratios for several wavelengths, can be obtained simultaneously. Such multichannel data are needed to simultaneously capture several aerosol properties such as concentration, size, and refractive index.

It is important to develop algorithms to retrieve aerosol properties from lidar data, as well as observation, because the information on the optical and microphysical properties of aerosols is essential for assessing the effects of aerosols on radiative impacts on the atmospheric environment and the lifetime of clouds in the climate system. Numerous aerosol retrieval algorithms from MSL data have been developed [3]–[7]. Algorithms that use data from both MSL and passive instruments have also been developed [8], [9]. Several algorithms using multichannel Raman lidar data have been developed [10]–[12]. Their algorithms retrieve the size distribution and complex refractive index of total aerosols. In order to assess atmospheric environments and climate change, it is necessary to identify aerosol components such as sulfate, black carbon, and dust and to determine their amounts. The methods developed by Sugimoto *et al.* [6], Nishizawa *et al.* [7], and Kaufman *et al.* [9] can classify aerosol types and estimate their concentrations. For example, the algorithm of Nishizawa *et al.* [7] estimates the extinction coefficients at $\lambda = 532$ nm for two kinds of aerosols, namely, water-soluble aerosols with sea salt and water-soluble aerosols with dust, at each slab layer by using dual-wavelength polarization MSL data. This algorithm was basically designed for analyzing the lidar data observed over the ocean. The data for the concentrations of the aerosol types retrieved by these algorithms can be a useful data set for validation and assimilation of aerosol transport models [13] because aerosol transport models generally simulate the movement or microphysical properties for each aerosol type.

In this paper, we develop a new algorithm for classifying aerosol types and estimating their extinction coefficients by using data from both HSRL and MSL. It estimates the extinction coefficients at $\lambda = 532$ nm for three types of aerosol components, namely, water soluble ($\sigma_{\mathrm{WS},532}$), soot ($\sigma_{\mathrm{ST},532}$), and dust ($\sigma_{\mathrm{DS},532}$), at each slab layer. We use four-channel data, comprising the extinction ($\sigma_{\mathrm{obs},532}$) and backscattering ($\beta_{\mathrm{obs},532}$) coefficients at $\lambda = 532$ nm derived from HSRL and the receiving signal ($P_{\mathrm{obs},1064}$)

Manuscript received November 13, 2007; revised April 18, 2008. Current version published November 26, 2008.

T. Nishizawa, N. Sugimoto, I. Matsui, A. Shimizu, and B. Tatarov are with the Atmospheric Environment Division, National Institute for Environmental Studies, Tsukuba 305-8506, Japan (e-mail: nisizawa@nies.go.jp).

H. Okamoto is with the Center for Atmospheric and Oceanic Studies, Graduate School of Science, Tohoku University, Sendai 980-8578, Japan.

Color versions of one or more of the figures in this paper are available online at http://ieeexplore.ieee.org.

Digital Object Identifier 10.1109/TGRS.2008.2000797

at $\lambda = 1064$ nm and total depolarization ratio ($\delta_{\mathrm{obs},532}$) at $\lambda = 532$ nm measured with MSL. Note that the algorithms of Müller *et al.* [10] and Veselovskii *et al.* [11] use eight and five observables at more wavelengths (i.e., 6 backscatter (β)+ 2 extinction (α) data and $2\alpha + 3\beta$ data), respectively, and Böckmann [12] proposed $3\beta + 1\alpha$ algorithm to retrieve aerosol optical properties from multichannel Raman lidar data. Our algorithm also requires four observables but with different combinations from Böckmann [12], i.e., $2\beta + 1\alpha + 1$ depolarization data. The algorithm was designed to analyze data collected by the ground-based HSRL and MSL of the National Institute for Environmental Studies (NIES). This algorithm focuses on main aerosol components over the land, and sea-salt aerosol is not treated, which is distinct from the method of Nishizawa *et al.* [7]. Except this difference, because we can use more information (four channels) compared with the previous study where we used three channels, it is expected that we can obtain more information in the new algorithm. Section II describes the relevant parameters and the methods used to obtain vertical profiles for the aerosol components. In Section III, we present an error analysis related to the measurement uncertainty. In Section IV, we demonstrate the ability of the developed algorithm by applying it to the observed data. Section V summarizes our findings.

II. Algorithm to Retrieve Aerosol Properties

A. Theoretical Formulas and Optical Properties of Aerosols Used in the Algorithm

The relation between the measured parameters, i.e., $\sigma_{\mathrm{obs},532}$, $\beta_{\mathrm{obs},532}$, and $P_{\mathrm{obs},1064}$, and the estimated parameters, i.e., $\sigma_{\mathrm{WS},532}$, $\sigma_{\mathrm{ST},532}$, and $\sigma_{\mathrm{DS},532}$, are represented by the following:

$$\sigma_{\mathrm{obs},532} = \sum_{i=1}^{3} \sigma_{i,532} \tag{1a}$$

$$\beta_{\mathrm{obs},532} = \sum_{i=1}^{3} \frac{\sigma_{i,532}}{S_{i,532}} \tag{1b}$$

$$P_{\mathrm{obs},1064} = C_{1064} \exp\{-2\tau_{1064}\}\left(\beta_{m,1064} + \sum_{i=1}^{3} V_i \sigma_{i,532}\right) \times \int_{Z_{q-1/2}}^{Z_{q+1/2}} \frac{1}{z^2} \exp\left\{-2(z - Z_{q-1/2}) \times \left(\sigma_{m,1064} + \sum_{i=1}^{3} W_i \sigma_{i,532}\right)\right\} dz. \tag{1c}$$

Subscript i means aerosol components, i.e., water soluble ($i = 1$), soot ($i = 2$), and dust ($i = 3$), and S is the lidar ratio. Equation (1c) is a modified discrete lidar equation [10], where Z_q is the altitude from the surface to the center of the qth slab layer. $Z_{q\pm1/2}$ is given by $Z_{q\pm1/2} = Z_q \pm \delta Z/2$, where δZ is the vertical resolution and C is a calibration constant. V and W are the ratios of backscattering and extinction coefficients at $\lambda = 1064$ nm to the extinction coefficient at $\lambda = 532$ nm (i.e., $V_i = \beta_{i,1064}/\sigma_{i,532}$, and $W_i = \sigma_{i,1064}/\sigma_{i,532}$). β_m and σ_m are the backscattering and extinction coefficients of the molecules. τ is the optical thickness of the molecules and aerosols from the surface to altitude $Z_{q-1/2}$. Equation (1) is a function of the following 16 unknown parameters: $\sigma_{i,532}$, $S_{i,532}$, V_i, W_i, τ_{1064}, C_{1064}, $\beta_{m,1064}$, and $\sigma_{m,1064}$ (where $i = 1$ to 3). To retrieve $\sigma_{i,532}$ at each slab layer from $\sigma_{\mathrm{obs},532}$, $\beta_{\mathrm{obs},532}$, and $P_{\mathrm{obs},1064}$, we must determine the other unknown parameters. The optical properties of the molecules, i.e., $\beta_{m,1064}$ and $\sigma_{m,1064}$, are obtained from atmospheric profiles of pressure and temperature given by radiosonde or an appropriate atmospheric model. τ_{1064} and C_{1064} can be determined by the method discussed in Section II-B. To determine the remaining parameters, namely, $S_{i,532}$, V_i, and W_i, we specify the microphysical properties such as size distribution and refractive index for each aerosol component. The values of $S_{i,532}$, V_i, and W_i are computed from the prescribed size distribution and refractive index for each aerosol component by using the Mie theory on the assumption that the aerosols are spherical and homogeneous. We utilize the values for the mode radius (r_m) and standard deviation (S_d) of the size distribution and the refractive index (m) for water-soluble, soot, and dust, as specified by the optical properties of aerosols and clouds (OPAC) in the algorithm. OPAC is a database of optical and microphysical properties of aerosols and clouds established by Hess *et al.* [15]. In OPAC, the size distribution for each aerosol component is assumed to be lognormal, and water-soluble aerosols are defined as particles consisting of various kinds of sulfates, organic compounds, and so on. The microphysical and optical properties of the aerosol components used in the algorithm are summarized in Table I. $S_{i,532}$ and V_i are key parameters in the estimation of $\sigma_{i,532}$ [see (1)]. If the values of $S_{i,532}$ and V_i for each aerosol component are similar, we cannot obtain an independent solution for $\sigma_{i,532}$ from $\sigma_{\mathrm{obs},532}$, $\beta_{\mathrm{obs},532}$, and $P_{\mathrm{obs},1064}$. As seen in Table I, the values of $S_{i,532}$ and V_i for each aerosol component differ considerably; for example, $S_{i,532}$ for soot is about twice and five times that for water-soluble components and dust, respectively, and V_i for dust is about 13 and 30 times as large as that for water-soluble components and soot. Hence, we can retrieve the extinction coefficients for each aerosol component at a given slab layer.

We computed the optical properties of dust by using the Mie theory and then made modification to account for the nonsphericity of dust particles. Raman lidar measurements revealed that the lidar ratio at $\lambda = 532$ nm was mostly between 42 and 55 sr for Asian dust [16] and mostly between 50 and 80 sr for Saharan dust [17], which are distinct from the typical value of 20 sr evaluated for spherical dust from the Mie theory [see Table I]. Liu *et al.* [16] and Müller *et al.* [17] suggested that the higher values of S_{532} obtained for Asian and Saharan dusts are caused mostly by nonsphericity of the particles. To consider the effect of nonsphericity of dust on the lidar ratio, we modified the optical properties for spherical dust evaluated from the Mie theory and created a new dust optical model (see "$\mathrm{Dust_M}$" in Table I). In the modified model, we assume that the dust lidar ratio at 532 nm is 50 sr and that the values of the spectral ratios of backscattering coefficients (i.e., $\beta_{\mathrm{DS},1064}/\beta_{\mathrm{DS},532}$)

TABLE I
MICROPHYSICAL AND OPTICAL PROPERTIES OF AEROSOL COMPONENTS ASSUMED IN THE ALGORITHM. THE VALUES OF THE MODE RADIUS (r_m), STANDARD DEVIATION (s_d), AND COMPLEX REFRACTIVE INDEX ($m_r - i\,m_i$) FOR THREE AEROSOL COMPONENTS ARE LISTED. THE OPTICAL PARAMETERS OF THE LIDAR RATIO (S_{532}), V, AND W FOR THE THREE AEROSOL COMPONENTS ARE CALCULATED BY THE MIE THEORY USING THE SIZE DISTRIBUTION AND COMPLEX REFRACTIVE INDEX. THE DUST OPTICAL MODEL Dust_S IS COMPUTED BY THE MIE THEORY AS SPHERICAL DUST. Dust_M IS A MODIFIED DUST OPTICAL MODEL THAT CONSIDERS THE EFFECT OF NONSPHERICITY OF DUST ON THE LIDAR RATIO. THE UNITS OF r_m, S, AND V ARE μm, sr, AND sr^{-1}, RESPECTIVELY

Property	Water-soluble	Soot	Dust_S	Dust_M
r_m	0.19	0.05	3.0	3.0
s_d	2.2	2.0	2.2	2.2
$m_{r,532}$, $m_{r,1064}$	1.44, 1.43	1.75, 1.76	1.53, 1.53	1.53, 1.53
$m_{i,532}$, $m_{i,1064}$	3×10^{-3}, 8×10^{-3}	4×10^{-1}, 4×10^{-1}	6×10^{-3}, 4×10^{-3}	6×10^{-3}, 4×10^{-3}
S_{532}	58	101	22	50
V	5.8×10^{-3}	2.3×10^{-3}	7.8×10^{-2}	3.4×10^{-2}
W	0.34	0.23	1.70	1.70

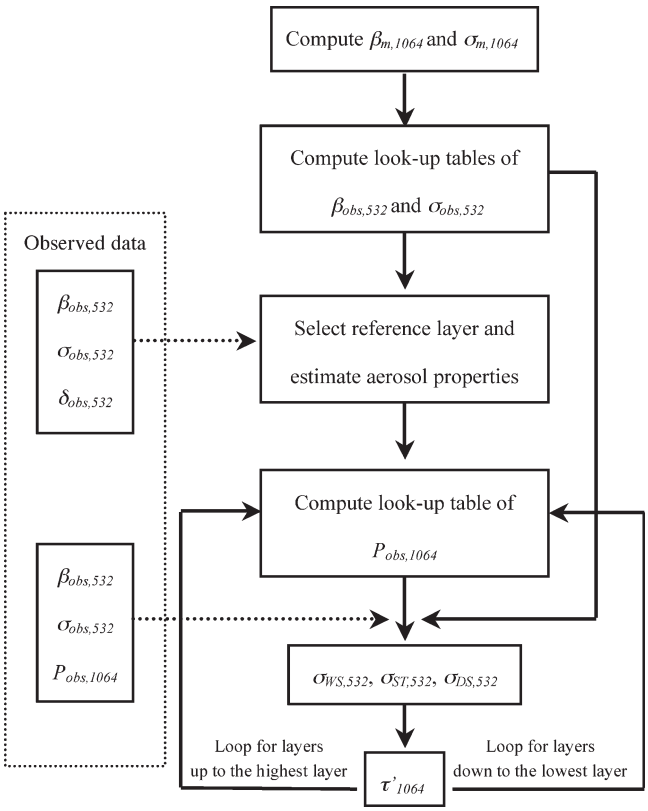

Fig. 1. Schematic diagram of the algorithm.

and extinction coefficients (i.e., $\sigma_{\text{DS},1064}/\sigma_{\text{DS},532}$) are the same as those for spherical dust.

B. Retrieve Vertical Profiles for Each Aerosol Component

The algorithm estimates the vertical profiles of $\sigma_{\text{WS},532}$, $\sigma_{\text{ST},532}$, and $\sigma_{\text{DS},532}$ that best reproduce the profiles of the observed $\sigma_{\text{obs},532}$, $\beta_{\text{obs},532}$, and $P_{\text{obs},1064}$. The retrieval procedure is shown schematically in Fig. 1. First, we calculate the molecular scattering using atmospheric profiles given by radiosonde or an appropriate atmospheric model, and we prepare a lookup table of $\sigma_{\text{obs},532}$ and $\beta_{\text{obs},532}$ as a function of $\sigma_{\text{WS},532}$, $\sigma_{\text{ST},532}$ and $\sigma_{\text{DS},532}$, where $\sigma_{\text{WS},532}$, $\sigma_{\text{ST},532}$, and $\sigma_{\text{DS},532}$ range from 0 to 1 km^{-1} every 0.001 km^{-1}. We then select one slab layer from all of the slab layers (hereafter referred to as the "reference layer") from which retrieval starts. The methods used to select the reference layer and to estimate the aerosol properties at the slab layer are described in the next section. After selecting the reference layer and estimating the aerosol properties at the layer, we repeated the following steps for each slab layer sequentially, from the reference layer up to the highest slab layer and down to the lowest slab layer.

1) Calculate a lookup table for the MSL signal at $\lambda = 1064$ nm$(P_{\text{obs},1064,l})$ by using (2), shown at the bottom of the next page.
2) Retrieve $\sigma_{\text{WS},532}$, $\sigma_{\text{ST},532}$, and $\sigma_{\text{DS},532}$ by using (3).
3) Retrieve the aerosol optical thickness from the reference layer to the given slab layer.

After retrieving the aerosol vertical profiles, we can evaluate C_{1064} and τ_{1064} by using the estimated $\sigma_{\text{WS},532}$, $\sigma_{\text{ST},532}$, and $\sigma_{\text{DS},532}$. In step 1), we calculate a lookup table for $P_{\text{obs},1064}$ as a function of $\sigma_{\text{WS},532}$, $\sigma_{\text{ST},532}$, and $\sigma_{\text{DS},532}$, which range from 0 to 1 km^{-1} every 0.001 km^{-1}, by using (2). $P_{\text{obs},1064}$ at the given slab layer can be computed by using the observed $P_{\text{obs},1064}$ and the retrieved $\sigma_{\text{WS},532}$, $\sigma_{\text{ST},532}$, and $\sigma_{\text{DS},532}$ at the reference layer in (2).

This equation is derived from (1c). Note that C_{1064} is canceled. The subscripts r and l refer to the reference layer and the lookup table, and τ'_{1064} is the aerosol optical thickness from the reference layer to the given slab layer. τ'_{1064} is computed in step 3), where we use the estimated values of σ_{WS}, σ_{ST}, and σ_{DS}. In step 2), we seek the combination of $\sigma_{\text{WS},532}$, $\sigma_{\text{ST},532}$, and $\sigma_{\text{DS},532}$, which minimizes the difference (D) between the observed and theoretical values (i.e., the values from the lookup table). D is defined as follows:

$$D = \left(\frac{\sigma_{\text{obs},532,l} - \sigma_{\text{obs},532}}{\sigma_{\text{obs},532}}\right)^2 + \left(\frac{\beta_{\text{obs},532,l} - \beta_{\text{obs},532}}{\beta_{\text{obs},532}}\right)^2 + \left(\frac{P_{\text{obs},1064,l} - P_{\text{obs},1064}}{P_{\text{obs},1064}}\right)^2 \quad (3)$$

where subscript l refers to the lookup table. We adopt the values of $\sigma_{\text{WS},532}$, $\sigma_{\text{ST},532}$, and $\sigma_{\text{DS},532}$, where the value of D is the smallest as the estimates for the slab layer. The maximum threshold value for D is set at 0.4.

C. Methods for Determining the Reference Layer

In this section, we discuss how we estimate aerosol properties at the reference layer and how we select the reference layer. First, we will discuss the method used to estimate aerosol properties at the reference layer. We select a reference layer where only two aerosol components or less are present so that the extinction coefficients at $\lambda = 532$ nm for two aerosol components are estimated from $\sigma_{\mathrm{obs},532}$ and $\beta_{\mathrm{obs},532}$ in the reference layer, which are directly obtained by HSRL. Note that $P_{\mathrm{obs},1064}$ is not calibrated at this stage in the retrieval. The following two aerosol models are assumed: Model 1 consists of water-soluble particles and soot, which are considered to be spherical particles, and model 2 consists of soot and nonspherical dust. We adopt model 1 (2) when the aerosol depolarization ratio $(\delta_{a,532})$ is smaller (or larger) than 0.1. After determining the model, we estimate the extinction coefficient of the two aerosol components for that model, e.g., $\sigma_{\mathrm{WS},532}$ and $\sigma_{\mathrm{ST},532}$ are estimated when model 1 is adopted. Note that the values of $\sigma_{\mathrm{WS},532}(\sigma_{\mathrm{DS},532})$ are set to be zero when $\delta_{a,532}$ is larger (or smaller) than 0.1. The procedure used here is a modified method from Nishizawa *et al.* [7], where three-channel data are measured with an MSL, i.e., backscattering data at 532 and 1064 nm (i.e., $P_{\mathrm{obs},532}$ and $P_{\mathrm{obs},1064}$) and total depolarization ratio (i.e., $\delta_{\mathrm{obs},532}$). They assume that the slab layer consists of spherical particles when $\delta_{a,532} < 0.1$ and that the slab layer includes dust, as well as spherical particles, when $\delta_{a,532} > 0.1$. They estimate extinction coefficients for two kinds of aerosol components from $P_{\mathrm{obs},532}$ and $P_{\mathrm{obs},1064}$. The aerosol depolarization ratio $(\delta_{a,532})$ is sensitive to the shape of the particles and is computed from $\delta_{\mathrm{obs},532}$ and $\beta_{\mathrm{obs},532}$ by using (4), shown at the bottom of the page. $\delta_{m,532}$ is the molecular depolarization ratio, which has an assigned value of 0.014 from the literature [18]. The $\delta_{a,532}$ value for spherical particles is zero. $\delta_{a,532}$ generally has a nonzero positive value for nonspherical particles (e.g., see [16], [19], and [20]).

Next, we describe the method used to select the reference layer. We avoid the case where the three aerosols, i.e., water-soluble particles, soot, and dust, are mixed. We locate a slab layer at which the value of $|\delta_{a,532} - 0.1|$ is maximal for all the slab layers and adopt that slab layer as the reference layer. Note that the value of $|\delta_{a,532} - 0.1|$ is larger, as spherical particles such as water-soluble components and soot become more dominant or as dust is more dominant; the value of $|\delta_{a,532} - 0.1|$ is close to zero when the spherical particles and dust are mixed.

III. Sensitivity Study on the Retrieval Errors in $\sigma_{\mathrm{WS},532}$, $\sigma_{\mathrm{ST},532}$, and $\sigma_{\mathrm{DS},532}$

We anticipated retrieval errors in $\sigma_{\mathrm{WS},532}$, $\sigma_{\mathrm{ST},532}$, and $\sigma_{\mathrm{DS},532}$ due to measurement uncertainty. We investigated the retrieval errors due to measurement bias to characterize the algorithm errors. In order to evaluate these errors, $\sigma_{\mathrm{obs},532}$, $\beta_{\mathrm{obs},532}$, $P_{\mathrm{obs},532}$, and $\delta_{\mathrm{obs},532}$ are first computed for a given model of aerosols and atmosphere. We then applied the algorithms to the simulated signals, with the measurement bias being equally added to all the ranges of the computed signals. We examined a situation in which water-soluble components and soot aerosols are concentrated in the lower layer and dust aerosols are present in the upper layer. To compute the $\delta_{\mathrm{obs},532}$ profile, aerosol depolarization ratios are assumed to be 0, 0, and 0.4 for water-soluble particles, soot, and dust, respectively. The midlatitude summer model published by McClatchey *et al.* [21] was used to calculate the optical properties of molecular scattering. The vertical resolution was set to 100 m. We considered the layer to lie between the altitudes of 0 and 5 km. Hereafter, we will express the retrieval error and the measurement uncertainty in terms of a parameter γ as $\delta\gamma = \gamma_c - \gamma_o$, where γ_o denotes a true value and γ_c corresponds to either a retrieved or a measured value. The relative error of γ is defined as $\Delta\gamma = \delta\gamma/\gamma_o$.

We consider the measurement uncertainties of $\pm 5\%$ for $\sigma_{\mathrm{obs},532}$. The constructed profiles for $\sigma_{\mathrm{WS},532}$, $\sigma_{\mathrm{ST},532}$, $\sigma_{\mathrm{DS},532}$, $\sigma_{\mathrm{obs},532}$, $\beta_{\mathrm{obs},532}$, and $P_{\mathrm{obs},1064}$ are shown in Fig. 2, with the aerosol optical thickness at $\lambda = 532$ nm being set to 0.3. We also present retrieved profiles for $\sigma_{\mathrm{WS},532}$, $\sigma_{\mathrm{ST},532}$, and $\sigma_{\mathrm{DS},532}$ and the extinction coefficient for total aerosols in the same figure. The magnitudes of the retrieval error for each aerosol component and total aerosols were smaller than 0.015 km^{-1} in extinction coefficient. The relative errors in the slab layers were smaller than 30%. $\Delta\sigma_{\mathrm{WS},532}$, $\Delta\sigma_{\mathrm{ST},532}$, and $\Delta\sigma_{\mathrm{DS},532}$ were 18%, 30%, and 4% at maximum.

$$P_{\mathrm{obs},1064,l} = P_{\mathrm{obs},1064,r} \exp\left\{-2\tau'_{1064}\right\} \times \frac{\left(\beta_{m,1064} + \sum_{i=1}^{3} V_i \sigma_{i,532}\right) \int_{Z_{l-1/2}}^{Z_{l+1/2}} \frac{1}{z^2} \exp\left\{-2(z - Z_{l-1/2})\left(\sigma_{m,1064} + \sum_{i=1}^{3} W_i \sigma_{i,532}\right)\right\} dz}{\left(\beta_{m,1064,r} + \sum_{i=1}^{3} V_i \sigma_{i,532,r}\right) \int_{Z_{l_r-1/2}}^{Z_{l_r+1/2}} \frac{1}{z^2} \exp\left\{-2(z - Z_{l_r-1/2})\left(\sigma_{m,1064,r} + \sum_{i=1}^{3} W_i \sigma_{i,532,r}\right)\right\} dz} \tag{2}$$

$$\delta_{a,532} = \frac{(1 + \delta_{m,532})\,\delta_{\mathrm{obs},532}\beta_{\mathrm{obs},532} + (\delta_{\mathrm{obs},532} - \delta_{m,532})\,\beta_{m,532}}{(1 + \delta_{m,532})\,\beta_{\mathrm{obs},532} - (\delta_{\mathrm{obs},532} - \delta_{m,532})\,\beta_{m,532}} \tag{4}$$

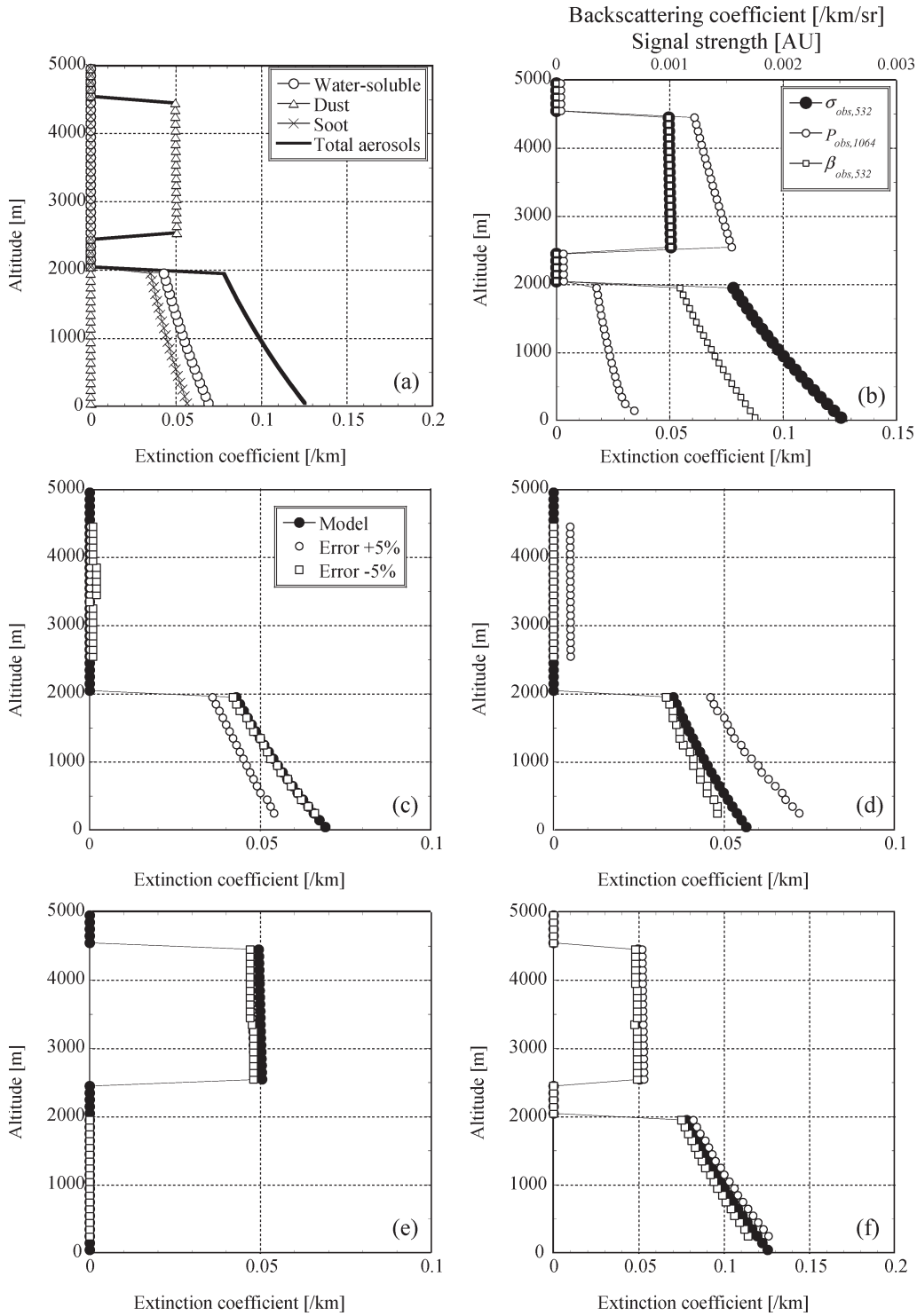

Fig. 2. Error analyses for a measurement uncertainty of $\pm 5\%$ for $\sigma_{\mathrm{obs},532}$. (a) The true vertical profiles of $\sigma_{\mathrm{WS},532}$, $\sigma_{\mathrm{ST},532}$, and $\sigma_{\mathrm{DS},532}$ and the extinction coefficient for total aerosols. (b) Constructed profiles for $\sigma_{\mathrm{obs},532}$, $\beta_{\mathrm{obs},532}$, and $P_{\mathrm{obs},1064}$. (c), (d), (e) and (f) Retrieved profiles for $\sigma_{\mathrm{WS},532}$, $\sigma_{\mathrm{ST},532}$, and $\sigma_{\mathrm{DS},532}$ and the extinction coefficient for total aerosols. The modified dust optical model ($\mathrm{Dust_M}$) was used in the error analysis.

We also investigated retrieval errors for $\Delta\beta_{\mathrm{obs},532}$ of $\pm 5\%$ and for $\Delta P_{\mathrm{obs},1064}$ of $\pm 5\%$. The results for $\Delta\beta_{\mathrm{obs},532} = \pm 5\%$ were similar to those for $\Delta\sigma_{\mathrm{obs},532} = \pm 5\%$: $\Delta\sigma_{\mathrm{WS},532}$, $\Delta\sigma_{\mathrm{ST},532}$, and $\Delta\sigma_{\mathrm{DS},532}$ were 23%, 28%, and 10% at maximum, respectively. The retrieval errors for $\Delta P_{\mathrm{obs},1064} = \pm 5\%$ were smaller than those for $\Delta\sigma_{\mathrm{obs},532}$ and $\Delta\beta_{\mathrm{obs},532}$ of $\pm 5\%$, i.e., 10%, 15%, and 7% for $\Delta\sigma_{\mathrm{WS},532}$, $\Delta\sigma_{\mathrm{ST},532}$, and $\Delta\sigma_{\mathrm{DS},532}$, respectively. We further investigated retrieval errors for $\Delta\sigma_{\mathrm{obs},532}$, $\Delta\beta_{\mathrm{obs},532}$, and $\Delta P_{\mathrm{obs},1064}$ of $\pm 10\%$, with $\Delta\sigma_{\mathrm{WS},532}$, $\Delta\sigma_{\mathrm{ST},532}$, and $\Delta\sigma_{\mathrm{DS},532}$, about twice those for $\Delta\sigma_{\mathrm{obs},532}$, $\Delta\beta_{\mathrm{obs},532}$, and $\Delta P_{\mathrm{obs},1064}$ of $\pm 5\%$. Note that the systematic measurement uncertainty for $P_{\mathrm{obs},1064}$ does not generate retrieval errors in $\sigma_{\mathrm{WS},1064}$, $\sigma_{\mathrm{ST},1064}$, and $\sigma_{\mathrm{DS},1064}$ since the bias for $P_{\mathrm{obs},1064}$ is canceled between the $P_{\mathrm{obs},1064}$

at the reference layer and that at the given slab layer. In this error analysis, we added the bias to computed $P_{\mathrm{obs},1064}$ in all the slab layers except at the reference layer.

We also investigated the sensitivity of the retrieval errors with regard to the assumptions for the algorithm. The microphysical and optical properties for each aerosol component in actual atmosphere vary in temporal and spatial [e.g., see [7] and references therein], but those are fixed in the algorithm (Table I); this simplification might affect the results. To examine the effects, we applied the algorithms to the constructed profiles of $\sigma_{\mathrm{obs},532}$, $\beta_{\mathrm{obs},532}$, and $P_{\mathrm{obs},1064}$ using the vertical profiles of $\sigma_{\mathrm{WS},532}$, $\sigma_{\mathrm{ST},532}$, and $\sigma_{\mathrm{DS},532}$ in Fig. 2(a), but using the optical properties of water-soluble particles with the mode radius of 0.14 μm, when $S_{\mathrm{WS},532}$ is 55 sr, instead of those with $r_{m,\mathrm{WS}}$ of 0.19 μm. Similarly, we also examined the cases for water-soluble particles with $r_{m,\mathrm{WS}}$ of 0.24 μm ($S_{\mathrm{WS},532} = 59$ sr), soot with $r_{m,\mathrm{ST}}$ of 0.1 μm ($S_{\mathrm{ST},532} = 109$ sr), and dust with $S_{\mathrm{DS},532}$ of 40 and 60 sr. The results showed that the relative errors in the slab layers were smaller than 5% in the cases for water-soluble particles with $r_{m,\mathrm{WS}}$ of 0.19 ± 0.05 μm. The retrieval errors for the soot ($r_{m,\mathrm{WS}} = 0.1$ μm) and dust ($S_{\mathrm{DS},532} = 50 \pm 10$ sr) cases were somewhat large, which were about 15% and 50%, respectively. The large retrieval errors in the dust case are partly due to retrieved aerosol optical properties at the reference layer. In all the cases, the slab layer at about 3 km, corresponding to the dust layer in the constructed model, was chosen as the reference layer. Thus, in the dust case, the difference of $S_{\mathrm{DS},532}$ between the algorithm and model causes the retrieval errors at the reference layer, and this affects the estimations at the other slab layers [see (2)]. When the reference layer is chosen at 1 km in the dust case, the retrieval errors reduce to 20%. We further examined the case that sea-salt particles, which are not considered in this algorithm, coexist. Sea-salt particles were added to the layer below 2 km in the aerosol profile in Fig. 2(a); the sea-salt optical thickness at $\lambda = 532$ nm is set to 0.05, and its optical properties ($r_{m,\mathrm{sea-salt}} = 1.5$ μm and $S_{\mathrm{sea-salt},532} = 25$ sr) are taken from OPAC. The results showed that the overestimation of water-soluble and dust particles and the underestimation of soot were found below 2 km: $\Delta\sigma_{\mathrm{WS},532}$ and $\Delta\sigma_{\mathrm{ST},532}$ reach 100% and -100%, respectively. However, the mixture might be rare because the data are taken over land.

IV. Application to HSRL and MSL Data

We applied our algorithm to the HSRL + MSL data measured at NIES located at 36.05° N and 140.12° E in Tsukuba, Japan, during March and April 2005, and we succeeded in determining the vertical structure for each aerosol component. The objective of this paper is not to show the results of the data analysis with the developed algorithm but rather to demonstrate the ability of the algorithm. We selected April 8, 2005, for analysis. On that day, plumes consisting of water-soluble components, soot, dust, or a mixture appeared; this situation is the best case for testing the developed algorithm. In the analysis, we used the midlatitude summer model published by McClatchey *et al.* [21] to calculate the optical properties of molecular scattering.

A. Observed Data Used in the Analysis

The MSL signals were recorded up to 24 km with 6-m resolution and every 10 s corresponding to 100 shots. The details of the MSL system can be found in [22]. The HSRL signals were recorded up to about 30 km with 3.75-m resolution and every 120 s (3600 shots). $\sigma_{\mathrm{obs},532}$ and $\beta_{\mathrm{obs},532}$ were derived from the raw data by averaging over 30 min in time and 150 m in range. The extinction measurements were restricted above 1 km. Details about the HSRL system and the derivation of $\sigma_{\mathrm{obs},532}$ and $\beta_{\mathrm{obs},532}$ can be found in [20].

We averaged the MSL data, i.e., $P_{\mathrm{obs},1064}$ and $\delta_{\mathrm{obs},532}$, every 150 m and 30 min in the vertical and temporal directions to match the temporal and vertical resolutions between the MSL and HSRL data. We used these values in the actual analysis. The retrieval of aerosol properties was limited to the layer from 1 to 6 km. The upper limit results from the signal-to-noise ratio of the MSL signals, and the lower limit results from the extinction measurements of HSRL.

B. Results of the Application

The observed data for April 8 suggest that three aerosol components, i.e., a water-soluble component (white solid lines), soot (black long-dashed lines), and dust (pink dash-dotted lines), might exist in Fig. 3 (hereafter, we refer to these areas as the white area, the black area, and the pink area, respectively). The lidar ratio ($S_{\mathrm{obs},532} = \sigma_{\mathrm{obs},532}/\beta_{\mathrm{obs},532}$) is very high (about 80 sr) in the black area, indicating the presence of soot. $\delta_{\mathrm{obs},532}$ is very high in the pink area (above 10%), indicating the presence of dust. In the white area, $S_{\mathrm{obs},532}$ is about 50 sr, and $\delta_{\mathrm{obs},532}$ is low (below 10%), indicating the presence of water-soluble aerosols. The estimated extinction coefficients for water-soluble particles and soot are higher in the white and black areas, respectively, than those in the other areas, and the water-soluble aerosols, soot, and dust mix in the white and black areas (Fig. 4). The mean extinction coefficients for water-soluble particles, dust, and soot in the black area are 0.02, 0.06, and 0.08 km^{-1}, which correspond to 12%, 38%, and 50% of the total extinction coefficient, respectively. In the white area, the mean extinction coefficient of water-soluble particles corresponds to 40% of the total extinction coefficient, which is comparable with the mean dust extinction coefficient. In the pink area, dust particles are dominant: Their mean extinction coefficient is more than 90% of the total extinction coefficient. Note that we use the modified dust optical model "Dust$_{\mathrm{M}}$" in this estimation. Dust particles seen in the black and white areas may be locally generated since the wind velocity measured at the surface on that day was relatively high from 0100 to 0900 UTC, ranging from 2 to 8 ms^{-1}, and the values of $P_{\mathrm{obs},1064}$ and $\delta_{\mathrm{obs},532}$ are very high below 2 km during that period. Dust particles in the pink areas may have been transported a long distance because the global aerosol transport model SPRINTARS [23] indicates that the dust comes from the Gobi desert in Mongolia. The water-soluble aerosols and soot in the black and white areas may have been transported long range because SPRINTARS indicates that the water-soluble aerosols and soot come from the Pacific seaboard of China/Indochina peninsula and the southern coastal region of China, respectively.

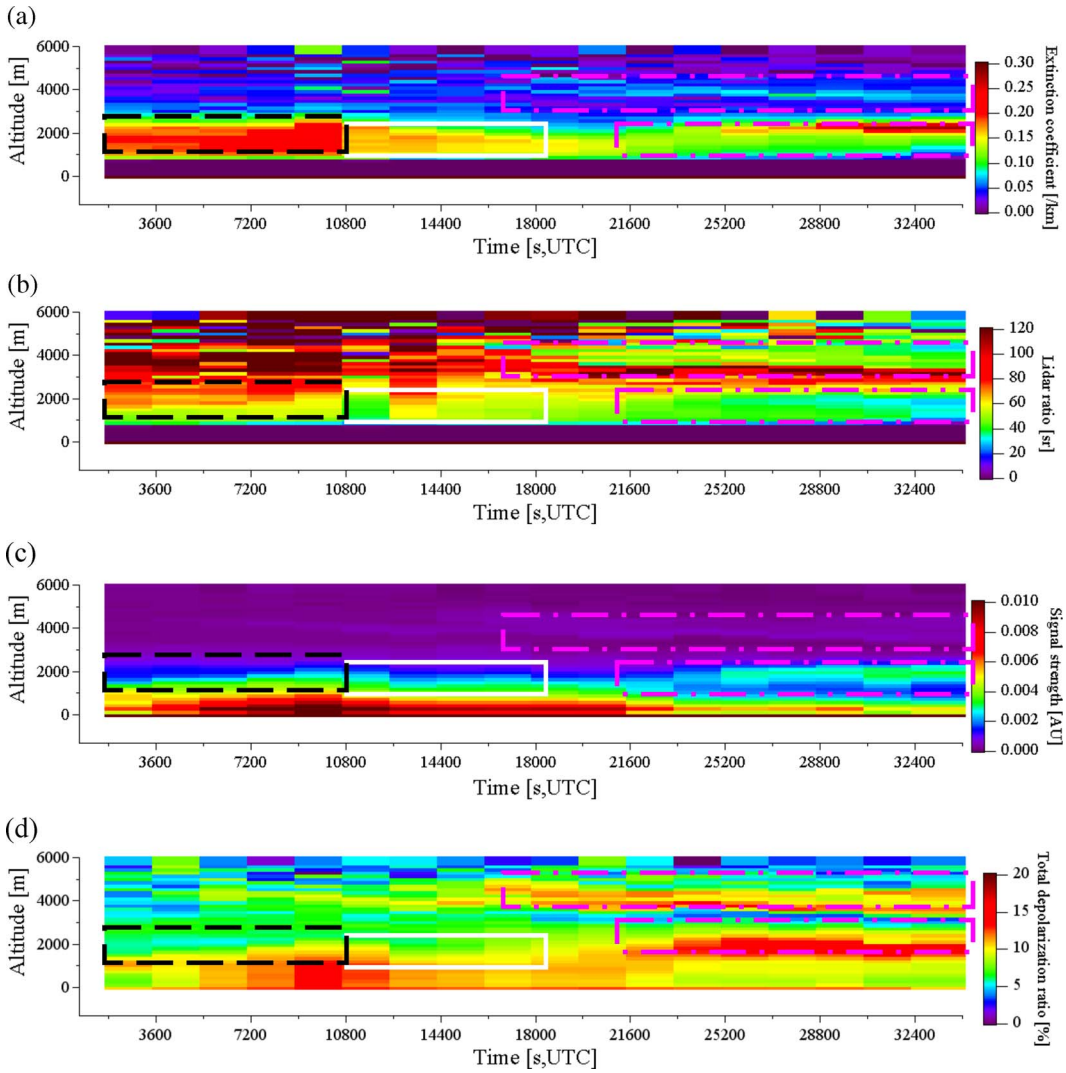

Fig. 3. Time–height cross sections of (a) $\sigma_{\mathrm{obs},532}$, (b) $S_{\mathrm{obs},532}$, (c) $P_{\mathrm{obs},1064}$, and (d) $\delta_{\mathrm{obs},532}$ measured on April 8, 2005.

We also applied the algorithm to the data for April 8 by using the spherical dust model "Dust$_{\mathrm{S}}$" (Fig. 5). The distribution patterns for each aerosol component roughly agree between the results for Dust$_{\mathrm{S}}$ and Dust$_{\mathrm{M}}$, although the estimates differ considerably. The values of $\sigma_{\mathrm{DS},532}$ with Dust$_{\mathrm{S}}$ are generally smaller because the lidar ratio of dust in Dust$_{\mathrm{S}}$ is smaller than that in the modified dust model "Dust$_{\mathrm{M}}$." $\sigma_{\mathrm{WS},532}$ and $\sigma_{\mathrm{ST},532}$ are larger for Dust$_{\mathrm{S}}$ because $\sigma_{\mathrm{WS},532}$ and $\sigma_{\mathrm{ST},532}$ must compensate for the reduction in $\sigma_{\mathrm{DS},532}$. We investigated the correlation between dust and $\delta_{a,532}$ to verify which results are more valid (Fig. 6). We found a positive correlation between the dust concentration for Dust$_{\mathrm{M}}$ and $\delta_{a,532}$ but could not find a positive correlation between the dust concentration for Dust$_{\mathrm{S}}$ and $\delta_{a,532}$. Thus, we conclude that the modified dust optical model provides more appropriate estimates than the spherical dust model.

V. Conclusion

We developed an algorithm to estimate the vertical profiles of extinction coefficients for water-soluble aerosols, soot, and dust by using the four-channel data from both HSRL and MSL, i.e., extinction and backscattering coefficients at 532 nm, backscattering data at 1064 nm, and total depolarization ratio at 532 nm. In the algorithm, the mode radii, standard deviations, and refractive indexes for each aerosol component were prescribed by the OPAC database, and their particles were assumed to be spherical and homogeneous; the optical properties for each aerosol component (Table I) were computed by the Mie theory. We implemented the nonsphericity of dust in the optical model, i.e., the dust lidar ratio at 532 nm was set to be 50 sr.

We demonstrated the ability of the algorithm by applying the algorithm to HSRL and MSL data measured at NIES on April 8, 2005. Plumes consisting of water-soluble aerosols, soot, dust, or their mixture were retrieved; these results were consistent with the results of simulation with SPRINTARS. We also performed an extensive sensitivity analysis and characterized the algorithm errors due to measurement uncertainty and the assumptions of the algorithm. From the aforementioned results, we suggest that the algorithm is a useful tool for capturing the temporal and vertical variations of aerosols. The results of the data analysis also indicated that the use of the modified dust optical model improved the estimates from the spherical dust optical model.

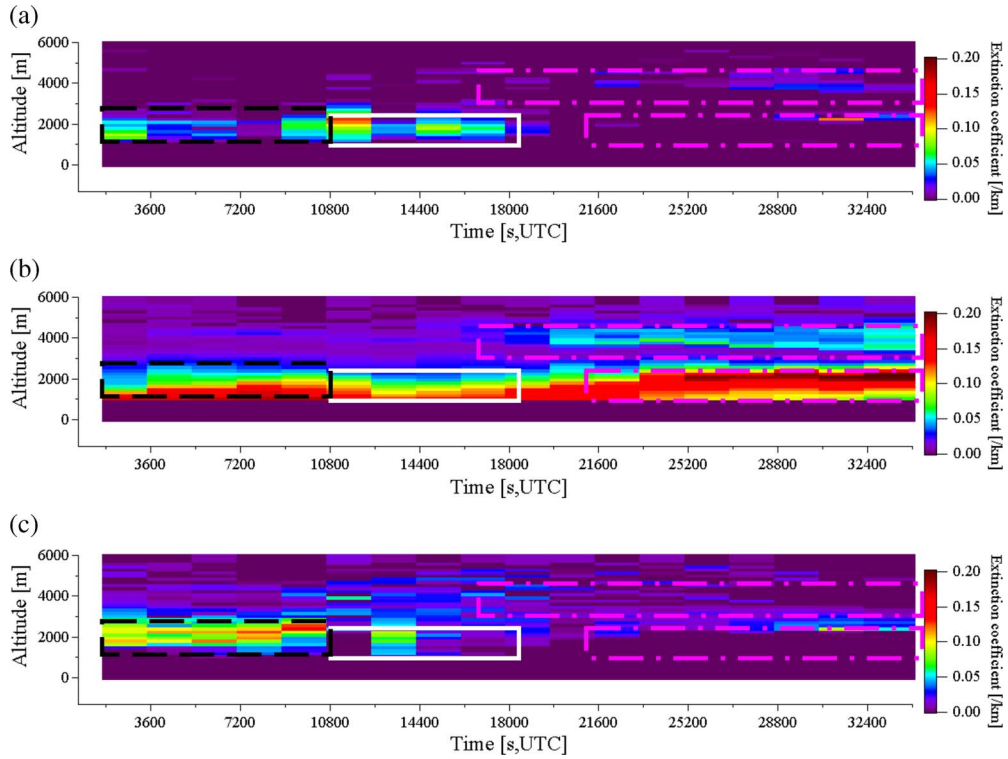

Fig. 4. Time–height cross sections of (a) $\sigma_{\mathrm{WS},532}$, (b) $\sigma_{\mathrm{DS},532}$, and (c) $\sigma_{\mathrm{ST},532}$ retrieved from data measured on April 8, 2005. The modified dust optical model ($\mathrm{Dust_M}$) was used in the retrieval.

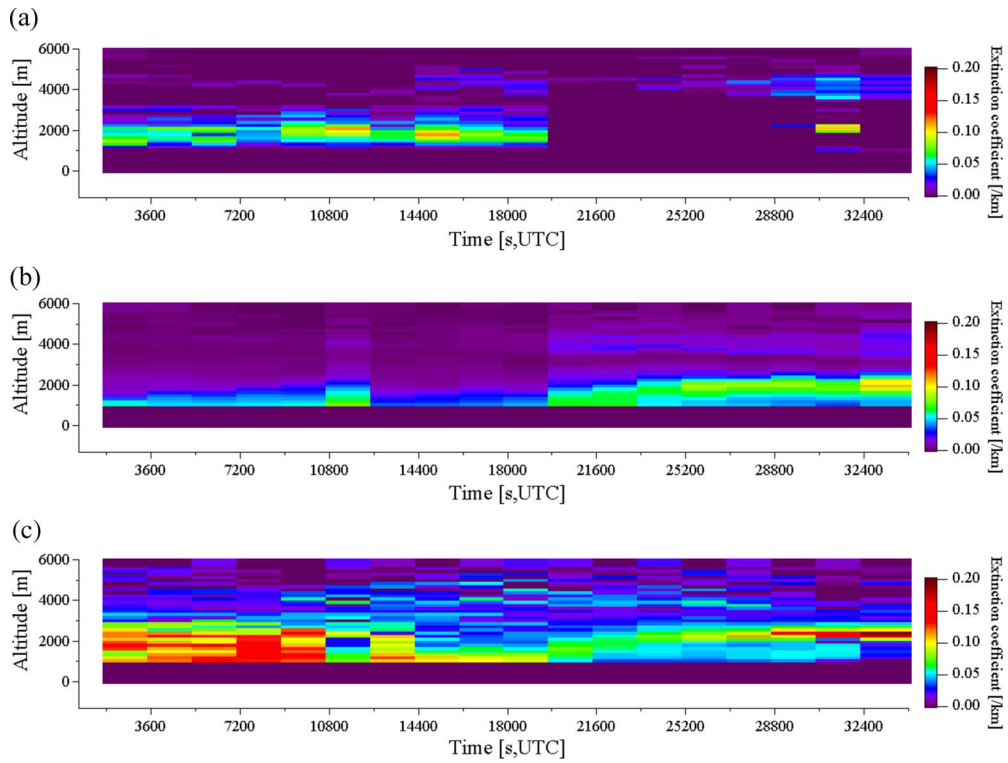

Fig. 5. Same as in Fig. 4, but with the spherical dust optical model ($\mathrm{Dust_S}$) used in the retrieval.

In this paper, we selected a typical case to test and demonstrate the ability of the algorithm. We will report the aerosol properties deduced from the application of the algorithm to the NIES lidar data over a longer period in a forthcoming paper. Spaceborne lidar measurements with HSRL at $\lambda = 355$ nm will be conducted beginning in 2012 in the spaceborne lidar and radar mission EarthCARE. We will develop an algorithm to retrieve aerosol properties from the HSRL data gathered by the EarthCARE satellite by modifying the algorithm developed in this paper.

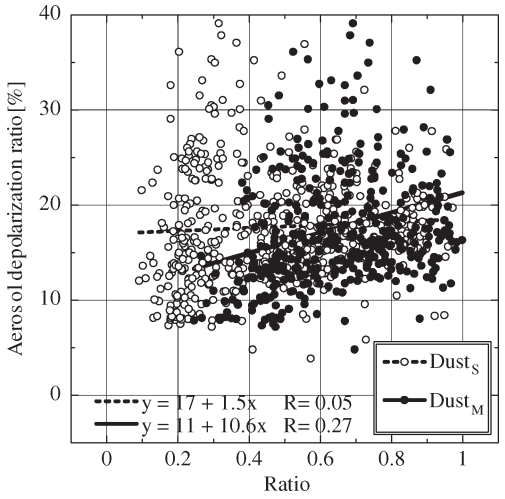

Fig. 6. Correlation between the aerosol depolarization ratio at $\lambda = 532$ nm($\delta_{a,532}$) and the ratio of backscattering coefficient at $\lambda = 532$ nm for dust ($\beta_{D,532}$) to that for total aerosols ($\beta_{T,532}$) (i.e., $\beta_{D,532}/\beta_{T,532}$). $\delta_{a,532}$, $\beta_{D,532}$, and $\beta_{T,532}$ are for April 8, 2005. The equation and correlation coefficient (R) for the line of regression are also shown in the figure.

ACKNOWLEDGMENT

The authors would like to thank Dr. A. Uchiyama of the Meteorological Research Institute for providing the data for wind velocity at the surface; Dr. T. Takemura of Kyusyu University, Fukuoka, Japan, for providing and discussing the data simulated by the global aerosol transport model SPRINTARS; and the anonymous reviewers for their useful comments.

REFERENCES

[1] Z. Liu, I. Matsui, and N. Sugimoto, "High-spectral-resolution lidar using an iodine absorption filter for atmospheric measurements," *Opt. Eng.*, vol. 38, no. 10, pp. 1661–1670, 1999.

[2] A. Ansmann, M. Riebesell, U. Wandinger, C. Weitkamp, and W. Michaelis, "Combined Raman elastic-backscatter LIDAR for vertical profiling of moisture, aerosol extinction, backscatter and LIDAR ratio," *Appl. Phys. B, Photophys. Laser Chem.*, vol. 55, no. 1, pp. 18–28, Jul. 1992.

[3] F. G. Fernald, "Analysis of atmospheric lidar observations: Some comments," *Appl. Opt.*, vol. 23, no. 5, pp. 652–653, May 1984.

[4] Y. Sasano and E. V. Browell, "Light scattering characteristics of various aerosol types derived from multiple wavelength lidar observations," *Appl. Opt.*, vol. 28, no. 9, pp. 1670–1679, May 1989.

[5] Z. Liu, P. Voelger, and N. Sugimoto, "Simulations of the observation of clouds and aerosols with the experimental lidar in space equipment system," *Appl. Opt.*, vol. 39, no. 18, pp. 3120–3137, Jun. 2000.

[6] N. Sugimoto, I. Uno, M. Nishikawa, A. Shimizu, I. Matsui, X. Dong, Y. Chen, and H. Quan, "Record heavy Asian dust in Beijing in 2002: Observations and model analysis of recent events," *Geophys. Res. Lett.*, vol. 30, no. 12, p. 1640, 2003. DOI: 10.1029/2002GL016349.

[7] T. Nishizawa, H. Okamoto, N. Sugimoto, I. Matsui, A. Shimizu, and K. Aoki, "An algorithm that retrieves aerosol properties from dual-wavelength polarization lidar measurements," *J. Geophys. Res.*, vol. 112, no. D6, p. D06 212, 2007. DOI: 10.1029/2006JD007435.

[8] T. Hayasaka, Y. Meguro, Y. Sasano, and T. Takamura, "Stratification and size distribution of aerosols retrieved from simultaneous measurements with lidar, a sunphotometer, and an aureolemeter," *Appl. Opt.*, vol. 37, no. 6, pp. 961–970, 1998.

[9] Y. J. Kaufman, D. Tanré, J.-F. Léon, and J. Pelon, "Retrievals of profiles of fine and coarse aerosols using lidar and radiometric space measurements," *IEEE Trans. Geosci. Remote Sens.*, vol. 41, no. 8, pp. 1743–1754, Aug. 2003.

[10] D. Müller, U. Wandinger, and A. Ansmann, "Microphysical particle parameters from extinction and backscatter lidar data by inversion with regularization: Theory," *Appl. Opt.*, vol. 38, no. 12, pp. 2346–2357, Apr. 1999.

[11] I. Veselovskii, A. Kolgotin, V. Griaznov, D. Muller, U. Wandinger, and D. N. Whiteman, "Inversion with regularization for the retrieval of tropospheric aerosol parameters from multiwavelength lidar sounding," *Appl. Opt.*, vol. 41, no. 18, pp. 3685–3699, 2002.

[12] C. Böckmann, "Hybrid regularization method for the ill-posed inversion of multiwavelength lidar data in the retrieval of aerosol size distributions," *Appl. Opt.*, vol. 40, no. 9, pp. 1329–1342, Mar. 2001.

[13] T. Nishizawa, H. Okamoto, T. Takemura, N. Sugimoto, I. Matsui, and A. Shimizu, "Aerosol retrieval from two-wavelength backscatter and one-wavelength polarizationlidar measurement taken during the MR01K02 cruise of the RV *Mirai* and evaluation of a global aerosol transport model," *J. Geophys. Res.*, 2008, accepted for publication.

[14] H. Okamoto, S. Iwasaki, M. Yasui, H. Horie, H. Kuroiwa, and H. Kumagai"An algorithm for retrieval of cloud microphysics using 95-GHz cloud radar and lidar," *J. Geophys. Res.*, vol. 108, no. D7, p. 4226, 2003. DOI: 10.1029/2001JD001225.

[15] M. Hess, P. Koepke, and I. Schult, "Optical properties of aerosols and clouds: The software package OPAC," *Bull. Amer. Meteorol. Soc.*, vol. 79, no. 5, pp. 831–845, 1998.

[16] Z. Liu, N. Sugimoto, and T. Murayama, "Extinction-to-backscatter ratio of Asian dust observed with high-spectral-resolution lidar and Raman lidar," *Appl. Opt.*, vol. 41, no. 15, pp. 2760–2767, 2002.

[17] D. Müller, I. Mattis, U. Wandinger, A. Ansmann, D. Althausen, O. Dubovik, S. Eckhardt, and A. Stohl, "Saharan dust over a central European EARLINET–AERONET site: Combined observations with Raman lidar and Sun photometer," *J. Geophys. Res.*, vol. 108, no. D12, p. 4345, 2003. DOI: 10.1029/2002JD002918.

[18] T. Murayama, H. Okamoto, N. Kaneyasu, H. Kamataki, and K. Miura, "Application of lidar depolarization measurement in the atmospheric boundary layer: Effects of dust and sea-salt particles," *J. Geophys. Res.*, vol. 104, no. D24, pp. 31 781–31 792, 1999.

[19] G. P. Gobbi, F. Barnaba, R. Giorgi, and A. Santacasa, "Altitude-resolved properties of a Saharan dust event over the Mediterranean," *Atmos. Environ.*, vol. 34, no. 29, pp. 5119–5127, 2000.

[20] B. Tatarov, N. Sugimoto, I. Matsui, and A. Shimizu, "Two-year-observations of optical properties of the tropospheric aerosol and clouds by a high-spectral-resolution lidar over Tsukuba, Japan," in Proc. 23rd Int. Laser Radar Conf., 2006, pp. 451–454.

[21] R. A. McClatchey, R. W. Fenn, J. E. A. Selby, F. E. Volz, and J. S. Garling, *Optical Properties of the Atmosphere*, 3rd ed. Bedford, MA: Air Force Cambridge Res. Lab., 1972. AFCRL Environ. Res. Pap., 411 108 pp.

[22] N. Sugimoto, I. Matsui, Z. Liu, A. Shimizu, I. Tamamushi, and K. Asai, "Observation of aerosols and clouds using a two-wavelength polarization lidar during the Nauru99 experiment," *J. Mar. Meteorol. Soc.*, vol. 76, no. 2, pp. 93–98, 2000.

[23] T. Takemura, T. Nozawa, S. Emori, T. Y. Nakajima, and T. Nakajima, "Simulation of climate response to aerosol direct and indirect effects with aerosol transport-radiation model," *J. Geophys. Res.*, vol. 110, no. D2, p. D02 202, 2005. DOI: 10.1029/2004JD005029.

Tomoaki Nishizawa received the B.S., M.S., and D.Sc. degrees in geophysics from Tohoku University, Sendai, Japan, in 1999, 2001 and 2004, respectively.

He was with Tohoku University, in 2004 and with the Meteorological Research Institute, Tsukuba, Japan from 2005 to 2006 as a Research Fellow of the Japan Society for the Promotion of Science. He is currently a Postdoc Fellow with the Atmospheric Environment Division, National Institute for Environmental Studies, Tsukuba. His research field is related to atmospheric environment and radiation budget. He is currently working on the development of algorithms to retrieve aerosol properties by using active optical remote sensing and data analysis using the developed algorithm.

Nobuo Sugimoto received the B.E. and M.E. degrees from Osaka University, Osaka, Japan, in 1976 and 1978, respectively, and the D.Sc. degree from the University of Tokyo, Tokyo, Japan, in 1985.

He has been with the National Institute for Environmental Studies (NIES), Tsukuba, Japan, since 1979. He is currently the Head of the Atmospheric Remote Sensing Section, Atmospheric Environment Division, NIES. He was the Leader of the science team for the Retroreflector in Space experiment in the ADEOS program in 1996. Also, he was the Leader of the team for data utilization study for NASDA's Experimental Lidar in Space Equipment. He is currently conducting observational studies using ground-based lidars and a shipboard lidar.

Ichiro Matsui received the B.Eng. degree from Hachinohe Institute of Technology, Hachinohe, Japan, in 1978, and the D.Eng. degree from Tohoku University, Sendai, Japan, in 1994.

He is currently a Senior Research Scientist with the Atmospheric Environment Division, National Institute for Environmental Studies, Tsukuba, Japan. He has been working on lidar techniques and atmospheric observations using lidars.

Atsushi Shimizu received the D.Sc. degree from the (former) Radio Atmospheric Science Center, Kyoto University, Kyoto, Japan.

He has been with the Atmospheric Environment Division, National Institute for Environmental Studies, Tsukuba, Japan, since December 1999.

Dr. Shimizu is currently a member of the Meteorological Society of Japan and the American Geophysical Union.

Boyan Tatarov received the M.S. degree in quantum electronics from Sofia University "St Kl. Okhridski," Sofia, Bulgaria, in 1995, and the Ph.D. degree from the Institute of Electronics, Bulgarian Academy of Sciences, Sofia, in 2002.

He was with the Institute of Electronics, Bulgarian Academy of Sciences, as a Research Associate from 2002 to 2003. He is currently a Postdoc Fellow with the Atmospheric Environment Division, National Institute for Environmental Studies, Tsukuba, Japan. His research field is related to lidar remote sensing of the atmosphere.

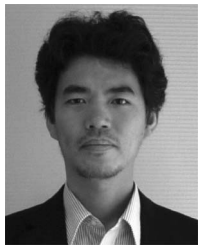

Hajime Okamoto received the B.S. degree in physics from Tokyo University of Science, Tokyo, Japan, in 1991, and the M.S. and D.Sc. degrees from Kobe University, Kobe, Japan, in 1993 and 1996, respectively.

He was a Japanese Society for the Promotion of Science Research Fellow with the Center for Climate System Research, University of Tokyo, Tokyo, from 1996 to 1998. He was with the Communications Research Laboratory between 1997 and 2001 as a researcher. He has been an Associate Professor with the Center for Atmospheric and Oceanic Studies, Graduate School of Science, Tohoku University, Sendai, Japan, since 2001.